Low-Potential Electrochemical Polymerization of 6-Nitroindole and Characterization of Its Polymers

Zhanggao Le,[1] Liqiang Zeng,[1] Jingkun Xu,[1,2] Houting Liu,[1] Mulin Ma[2]

[1]*Key Laboratory of Nuclear Resources and Environment of the Ministry of Education, East China Institute of Technology, 56 Xuefu Road, Fuzhou 344000, China*
[2]*Jiangxi Key Laboratory of Organic Chemistry, Jiangxi Science and Technology Normal University, Nanchang 330013, China*

Received 15 May 2007; accepted 23 September 2007
DOI 10.1002/app.27388
Published online 15 November 2007 in Wiley InterScience (www.interscience.wiley.com).

ABSTRACT: Conducting polymers bearing nitro substituents are very important from both academic and industrial viewpoints. However, it is very difficult to electrosynthesize such conducting polymers because of the strong electron-withdrawing effect of nitro groups. In this article, we describe the electrochemical synthesis of films of a new conducting polymer, high-quality poly(6-nitroindole) (P6NI), by direct anodic oxidation of 6-nitroindole in boron trifluoride diethyl etherate containing 10% (v/v) diethyl ether. The oxidation potential onset of 6-nitroindole in this medium has been measured to be just 0.98 V versus a saturated calomel electrode (SCE), which is much lower than that determined in acetonitrile containing 0.1 mol/L tetrabutylammonium tetrafluoroborate (1.6 V vs SCE). Thermal studies have revealed that P6NI displays good thermal stability. The electrical conductivity of the P6NI films has been measured to be 0.08 S/cm. Structural studies have shown that the polymerization of the 6-nitroindole ring occurs mainly at the 2,3-positions. Fluorescence spectral studies have shown that the principal excitation and emission peaks of P6NI are at 416 and 535 nm, respectively, with a fluorescence quantum yield of 0.05. All these properties of P6NI films may facilitate their potential applications in various fields, such as electrochemical sensors and green-light-emitting materials. To the best of our knowledge, this is the first report on the electrosynthesis and characterization of 6-nitro-substituted polyindole films. © 2007 Wiley Periodicals, Inc. J Appl Polym Sci 107: 2793–2801, 2008

Key words: conducting polymers; conjugated polymers; electrochemistry; films

INTRODUCTION

The pursuit of high-quality films of conducting polymers is still one of the main goals in the research and development of inherently conducting polymers[1–4] because of their potential applications in rechargeable batteries, electrochromic display devices, supercapacitors, antistatic coatings, biosensors, and so forth. Electro-oxidative deposition has been proven to be an especially useful approach for the preparation of electroactive and conducting polymer films.[5,6] Among the conducting polymers investigated during the past quarter century, polyindole and its derivatives have attracted significant attention[7–32] because of their fairly good thermal stability, high redox activity and stability,[11–14] slow degradation rate in comparison with those of polyaniline and polypyrrole,[13] and air-stable electrical conductivity in the doped state.[15] Polyindole may be a good candidate for applications in electrochemical sensors, electrocatalysis, mild steel protection,[33] and biological areas. For many of these applications, it is desirable to produce electroactive polyindole layers with a wide variety of substituents.

On the other hand, the band gap of conducting polymers is a very crucial factor for improving the properties of semiconductors; it is the difference in energy between the valence band [highest occupied molecular orbital (HOMO)] and the conduction band [lowest unoccupied molecular orbital (LUMO)].[34] Intrinsic conductors owe their conductivity to a partial filling of the valence band up to the Fermi level. To imitate such a partially filled band with a semiconductor, the band gap should be zero or close to zero. In semiconductors, the valence and conduction bands are curved by space-charge effects, which lead to a diminished band-gap energy when the spatial alternation of the levels is taken into account. Conducting polymers are usually semiconductors. There-

Correspondence to: J. Xu (xujingkun@tsinghua.org.cn or xujingkun@mail.ipc.ac.cn).

Contract grant sponsor: National Science Foundation of China; contract grant number: 50663001.
Contract grant sponsor: Funds of the Ministry of Education of China; contract grant number: 2007-20758.
Contract grant sponsor: Funds of the Key Laboratory of Nuclear Resources and Environment of the Ministry of Education, East China Institute of Technology; contract grant number: 060606.

fore, the lower the band gap is, the better the electrical conductivities of conducting polymers are likely to be. One of the most intriguing properties of conducting polymers is that their band gaps can be tuned by substituents on the conjugated main chain. Generally, substitution with electron-donating (donor) groups increases the HOMO level, whereas substitution with electron-withdrawing (acceptor) groups decreases the LUMO level. Thus, the high-lying HOMO of the donor fragment and the low-lying LUMO of the acceptor fragment can yield an unusually small HOMO–LUMO separation,[35,36] leading to a smaller band gap. Previous studies have mainly been concerned with donor-group-substituted conducting polymers, such as poly(3,4-ethylenedioxythiophene)[6,37] and poly(3-methylthiophene).[38,39] However, there have been very few reports on conducting polymers bearing electron-withdrawing groups because these render the formation of conducting polymer films very difficult.

It has been reported that nitro group substitution on conducting polymers can diminish their band gap because of the strong electron-withdrawing substituent effect.[34] Nitro group substitution on the conjugated backbone of conducting polymers has several other advantages. First, the nitro group itself can be reduced during redox processes of the corresponding conducting polymers. Because its reduction consumes many electrons, conducting polymers bearing nitro groups could probably be used in electrochemical batteries in which the charge storage would be faradaic in nature rather than capacitive.[40] Second, a nitro group on the main backbone can be easily reduced to an amido group, which will further improve the properties of inherently conducting polymers; third, the introduction of nitro groups onto the main backbone of conducting polymers will also provide a novel approach for the postfunctionalization of inherently conducting polymers through the reduction of NO_2 to NH_2. Thus, an investigation of the syntheses and characterization of conducting polymers substituted with nitro groups was deemed necessary. However, substitution of conducting polymers with strongly electron-withdrawing nitro groups usually leads to a higher oxidation potential of the corresponding monomer and poorer polymer film quality. It has been reported that a strongly destabilizing nitro substituent inhibits electropolymerization, and almost no conducting polymer films can be formed, mainly because the strongly electron-withdrawing nitro group sufficiently stabilizes the radical cation intermediates such that these diffuse away from the electrode and no further reactions can take place on the anode surface.[20]

Boron trifluoride diethyl etherate (BFEE) is an excellent electrolyte, and no other supporting electrolyte is needed for the electrochemical polymerization of aromatic compounds, such as benzene and thiophene, in this medium.[40–45] High-quality conducting polymer films can be generated in this electrolyte. Our previous studies have shown that freestanding high-quality polyindole films can also be prepared from BFEE,[46] in analogy to other high-quality conducting polymer film formations in this medium, such as those of polythiophenes,[47] polypyrrole,[48] polyfuran,[49,50] and poly(*para*-phenylene).[51] To date, there have been no reports on the electropolymerization of 6-nitroindole in BFEE-based electrolytes.

In this study, poly(6-nitroindole) (P6NI) films have easily been prepared by direct anodic oxidation of 6-nitroindole monomer in BFEE containing 10% diethyl ether (EE). The electrochemical properties, polymerization mechanism, thermal stability, fluorescent properties, and morphology of the as-prepared P6NI films have been studied in detail.

EXPERIMENTAL

Materials

BFEE (Beijing Changyang Chemical Plant, Beijing, China) was distilled and stored at −20°C before use. 6-Nitroindole (Acros Organics, NJ) and commercial high-performance liquid chromatography grade acetonitrile (CH_3CN; Tianjin Kermel Chemical Reagents Research Institute, Tianjing, China) were used as received. Tetrabutylammonium tetrafluoroborate (Bu_4NBF_4; 95%; Acros Organics, NJ) was dried *in vacuo* at 60°C for 24 h before use. Tetrahydrofuran (THF; analytical grade) was obtained from Beijing Chemical Plant (Beijing, China). Perdeuterated dimethyl sulfoxide (DMSO-d_6) was a product of Cambridge Isotope Laboratories, Inc (Andover, MA).

Electrosyntheses of P6NI films

Electrochemical syntheses and examinations were performed in a one-compartment cell with a model 263 potentiostat/galvanostat (EG&G Princeton Applied Research, OakRidge, TN) under computer control. For electrochemical examinations, the working and counter electrodes were a Pt wire with a diameter of 0.5 mm and a stainless steel wire with a diameter of 1 mm, respectively. They were placed 5 mm apart during the experiments. To obtain a sufficient amount of polymer for characterization, stainless steel sheets with respective surface areas of 10 and 12 cm^2 were employed as the working and counter electrodes, respectively. According to the literature,[52–54] the use of Pt or stainless steel sheets has little impact on the electrochemical polymerization. The aforementioned electrodes were carefully polished with abrasive paper (1500 mesh) and then successively cleaned with water and acetone before

each examination. All potentials were referred to a saturated calomel electrode (SCE).

A typical electrolytic solution consisted of BFEE containing 10% EE and 0.02 mol/L 6-nitroindole. The amount of polymer film deposited on the electrode was controlled by the integrated current that passed through the cell. To remove the electrolyte, oligomers, and monomer, the electropolymerized films were rinsed with acetone and pure water. As-formed P6NI films were obtained in the doped state and were dark metallic in color. For spectral analysis, the polymer was dedoped with 25% ammonia for 3 days and then washed repeatedly with water. Finally, it was dried *in vacuo* at 60°C for 24 h.

Characterization

The electrical conductivities of the as-formed P6NI films were measured by the application of a conventional four-probe technique. Ultraviolet–visible (UV–vis) spectra were measured with a PerkinElmer Lambda 900 UV–vis/near-IR spectrophotometer (Waltham, MA). IR spectra were recorded with a Nicolet 510P Fourier transform infrared (FTIR) spectrometer (Waltham, MA) with samples in KBr pellets. Fluorescence spectra were determined with an F-4500 fluorescence spectrophotometer (Hitachi, Tokyo, Japan). ^{1}H-NMR spectra were recorded on a Bruker AV 400 NMR spectrometer (Fallanden, Switzerland) with DMSO-d_6 as the solvent. Thermogravimetric analysis (TGA) was performed with a Pyris Diamond thermogravimetry/differential thermal analysis thermal analyzer (PerkinElmer, Waltham, MA). Scanning electron microscopy (SEM) measurements were made with a JEOL JSM-6700F scanning electron microscope (Tokyo, Japan). The fluorescence quantum yield ($\phi_{overall}$) of the soluble P6NI samples was measured to be 0.05 with anthracene in CH_3CN [standard; reference quantum yield (ϕ_{ref}) = 0.27][55] as a reference and was calculated according to the well-known method based on the following expression:

$$\phi_{overall} = \frac{n^2 A_{ref} I}{n_{ref}^2 A I_{ref}} \times \phi_{ref} \quad (1)$$

where n, A, and I denote the refractive index of the solvent, the absorbance at the excitation wavelength, and the intensity of the emission spectrum, respectively. The absorbances of the samples and the standard should be similar.[56,57]

RESULTS AND DISCUSSION

Electrochemical syntheses of P6NI films

Figure 1 shows the anodic polymerization curves of 6-nitroindole in mixed electrolytes of BFEE containing different amounts of EE. The oxidation onset of 6-nitroindole was initiated at 0.98 V versus SCE in pure BFEE [Fig. 1(A)]. The addition of 10, 30, and 50% EE to BFEE significantly increased the onset oxidation potential of the monomer to about 0.99, 1.06, and 1.13 V, respectively [Fig. 1(B–D)]. All these values are much lower than that of 6-nitroindole in CH_3CN containing 0.1 mol/L Bu_4NBF_4 (1.6 V), as shown in the inset in Figure 1. Furthermore, no film was observed on the electrode surface after linear sweep voltammetry in the medium of CH_3CN containing 0.1 mol/L Bu_4NBF_4. From this point of view, pure BFEE is the electrolyte of choice because, in general, a lowering of the monomer oxidation potential onset can prevent side reactions and lead to higher quality polymer films. On the other hand, the addition of a small amount of EE to pure BFEE has several advantages. Additional EE can improve the solubility of the monomer in the mixed electrolyte; 6-nitroindole is poorly soluble in pure BFEE but dissolves readily in EE. Moreover, at a given applied potential, the higher the current density is during oxidation, the faster the polymerization rate will be. Thus, the addition of a small amount of EE can accelerate the polymerization reaction [Fig. 1(B)]. According to Figure 1, the oxidation potential of the monomer increased with increasing EE content in the mixed electrolyte. Higher oxidation potentials usually lead to side reactions during the polymerization process and thus result in poor polymer film quality.[40,58,59] In Figure 1, the current density of the anodic polarization curve in the medium of CH_3CN containing 0.1 mol/L Bu_4NBF_4 is seen to be almost 4 times higher than in the mixed media of BFEE containing different amounts of EE. The origin of this phenomenon is usually attributed to the low conduc-

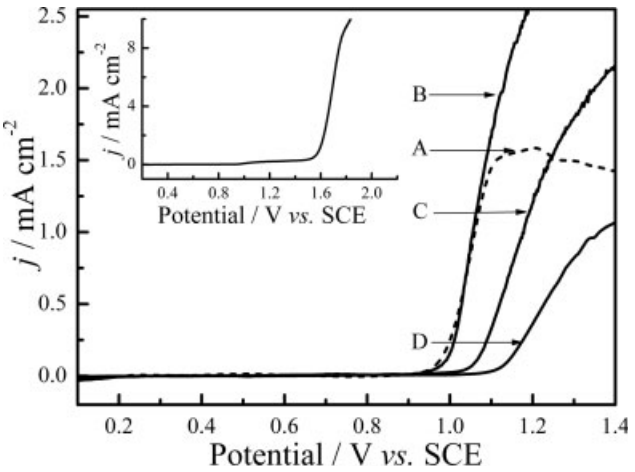

Figure 1 Anodic polarization curves of 6-nitroindole in mixed electrolytes of BFEE containing (A) 0, (B) 10, (C) 30, and (D) 50% EE (v/v) and in CH_3CN containing 0.1 mol/L Bu_4NBF_4 (inset). The potential scanning rate was 20 mV/s; j is the current density.

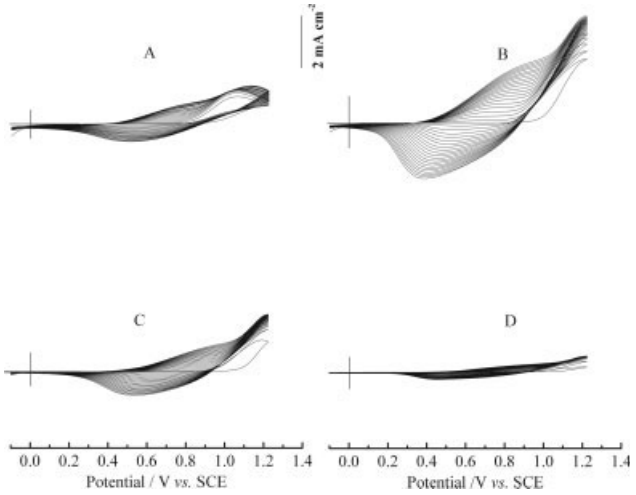

Figure 2 Cyclic voltammograms of 0.02 mol/L 6-nitroindole in (A) pure BFEE and in mixed electrolytes of BFEE containing (B) 10, (C) 30, and (D) 50% EE. The potential scanning rate was 100 mV/s.

tivity of BFEE (generally ca. 400 μS/cm), which leads to a diffusion-controlled electrochemical process. On the basis of these considerations, the mixed electrolyte for the electrosynthesis of P6NI was chosen to be BFEE containing 10% EE.

Successive cyclic voltammograms of 0.02 mol/L 6-nitroindole in the mixed electrolyte on a Pt electrode are shown in Figure 2. As can be seen in Figure 2(A), the cyclic voltammograms of 6-nitroindole in pure BFEE show the characteristic features of other conducting polymers such as polypyrrole and polythiophene during the potentiodynamic syntheses. As the cyclic voltammetry scans continued, a polymer film was formed on the Pt electrode surface. P6NI can be reduced and oxidized between 0.5 and 0.9 V. The increase in the redox wave currents of the polymer implied that the amount of polymer on the electrode increased. The potential shift of the current wave maximum provides information about the increase in the electrical resistance of the polymer film and the overpotential needed to overcome this resistance.[60] When EE was added to BFEE, a similar phenomenon could be observed [Fig. 2(B–D)]. It can also be seen in Figure 2 that the increase in the redox wave current densities per cycle was highest in BFEE containing 10% EE [Fig. 2(B)]. As the EE content in the mixed electrolyte was further increased, this increase per cycle decreased. This may be ascribed to the fact that the oxidation potential of the monomer increased with increasing EE concentration [Fig. 1(B–D)]. According to the electrochemical kinetics, at a given applied potential (E), the polymerization rate depends exponentially on the potential difference ($E - E^0$) between E and the oxidation potential of the monomer (E^0). The addition of EE increases E^0 of the monomer. Thus, with increasing EE content, the polymerization rate decreased at a given applied potential. This resulted in the phenomena shown in Figure 2(B–D). Therefore, in all subsequent work, we focused on electrosyntheses and characterizations of P6NI films prepared in BFEE containing 10% EE.

The electrochemical behavior of the P6NI films deposited electrochemically from BFEE containing 10% EE was studied in monomer-free BFEE containing 10% EE [Fig. 3(A)] and in CH_3CN containing 0.1 mol/L Bu_4NBF_4 [Fig. 3(B)]. Similar to results reported previously in the literature,[12] the steady-state cyclic voltammograms displayed broad anodic and cathodic peaks. Two anodic peaks were seen at a slow scanning rate of 50 mV/s [Fig. 3(A)]. These anodic peaks were centered at 0.91 and 1.18 V and can mainly be ascribed to oxidation of the short-chain polymer. When the scanning rate was increased, these peaks were no longer resolved,

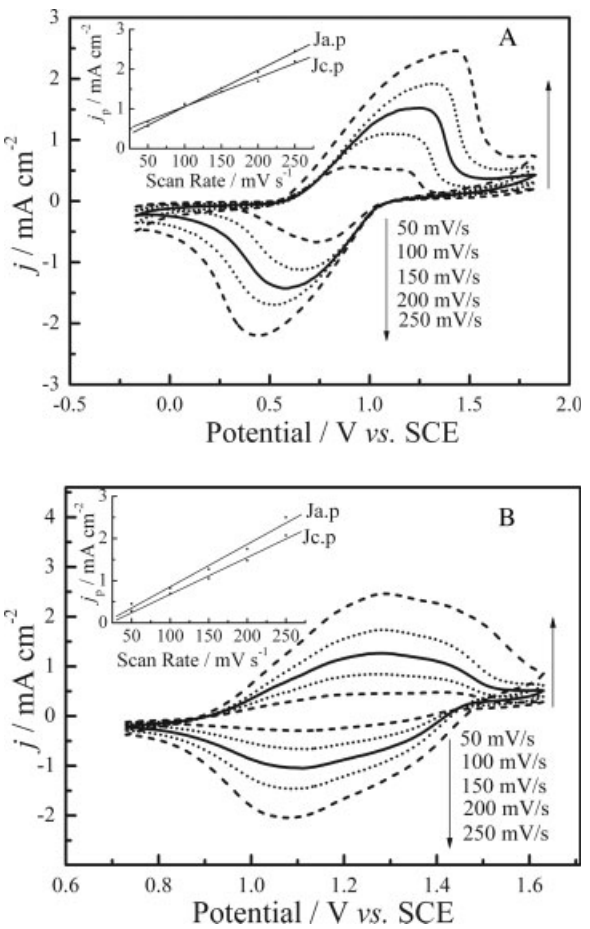

Figure 3 Cyclic voltammograms of a P6NI film in (A) BFEE containing 10% EE and (B) CH_3CN containing 0.1 mol/L Bu_4NBF_4 at potential scanning rates of 50, 100, 150, 200, and 250 mV/s. The P6NI film was synthesized electrochemically in BFEE containing 10% EE at a constant applied potential of 1.23 V versus SCE. j is the current density, and $J_{a,p}$ and $J_{c,p}$ denote the anodic and cathodic peak current densities, respectively.

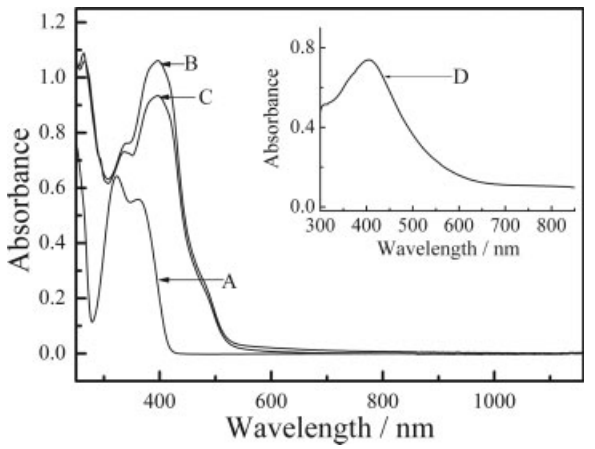

Figure 4 UV–vis spectra of (A) 6-nitroindole, (B) doped P6NI, and (C) dedoped P6NI prepared from BFEE containing 10% EE (v/v) and 0.02 mol/L 6-nitroindole at a constant applied potential of 1.23 V versus SCE. The solvent was THF. (D) The inset shows the UV–vis spectrum of a doped P6NI film on an ITO electrode.

mainly because scanning was faster than the oxidation of the short-chain polymer. The peak current densities are proportional to the scan rates [insets in Fig. 3(A,B)], and this indicates reversible redox behavior of the polymer. Furthermore, these films could be repeatedly cycled between the conducting (oxidized) and insulating (neutral) states without significant decomposition, and this indicates the high stability of the polymer. The polymer film could be oxidized and reduced from 1.44 to 0.41 V in BFEE containing 10% EE [Fig. 3(A)] and from 1.28 to 1.07 V in CH_3CN containing 0.1 mol/L Bu_4NBF_4 [Fig. 3(B)]. All these results indicate that the as-formed P6NI films had good redox activity and stability.

Structural characterization

As-prepared doped P6NI films obtained from BFEE containing 10% EE were dark metallic in color. When they were dedoped with 25% ammonia, little color change was noted. Doped and dedoped P6NIs were found to be partly soluble in dimethyl sulfoxide and THF but almost insoluble in CH_3CN. Therefore, the UV–vis spectra of the monomer 6-nitroindole, as well as doped and dedoped P6NI, were examined in THF. As shown in Figure 4, the monomer showed several characteristic absorptions at 320 and 360 nm [Fig. 4(A)]. The doped and dedoped P6NI films showed much broader absorptions, with several fine structures at 264, 338, and 396 nm. The UV–vis absorption spectra of the doped and dedoped films in THF extended to 550 nm. The redshift of the UV–vis spectra of P6NI reflects the higher conjugation of the backbone in comparison with the monomer.[61] Similar absorptions were noted in the UV–vis spectra of both doped and dedoped P6NI and were possibly due to an automatic dedoping process of P6NI in the THF solution. Furthermore, the doped P6NI film showed another strong absorption on an indium tin oxide (ITO) electrode from 320 to 660 nm, with a peak centered at about 400 nm [Fig. 4(D)]. This broad peak can be assigned to the absorption of conductive species on the main backbone of P6NI in the doped state.[57]

Vibrational spectra can provide structural information on neutral and doped conducting polymers. A comparison of the evolution of the vibrational modes appearing in conducting polymers and in some simpler related molecules serving as references usually aids the interpretation of the experimental absorption spectra. For polyindole and its derivatives, the vibrational spectra are particularly useful because they may be used to interpret the polymerization mechanism. According to the literature, there are two main opinions regarding the positions involved in the electrochemical polymerization mechanism of indole and its derivatives: the 1,3-positions[62] and the 2,3-positions.[18,28,63] The presence or absence of the N—H vibration mode in the spectrum of the doped P6NI is the key factor for determining whether the polymerization involves a reaction at the 1-position.

Figure 5 displays the transmittance FTIR spectra of 6-nitroindole monomer [Fig. 5(A)] and doped P6NI [Fig. 5(B)]. Details of the band assignments of the monomer and the doped P6NI are given in Table I. The strong and narrow peak at 3332 cm^{-1} observed in the spectrum of 6-nitroindole is the characteristic absorption of the N—H bond, which is broader and shifts to 3351 cm^{-1} in the spectrum of the doped P6NI film. This band, together with the band at 1585 cm^{-1}, can be ascribed to elongation and deformation vibrations of the N—H bond, respectively. This result implies that there were still

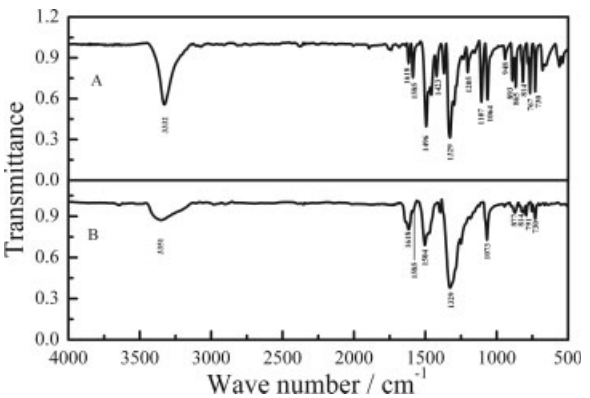

Figure 5 FTIR spectra of (A) 6-nitroindole monomer and (B) a doped P6NI film. Doped P6NI films were obtained potentiostatically at 1.23 V versus SCE from BFEE containing 10% EE.

TABLE I
Assignments of the IR Spectra of the Monomer and Doped P6NI

Band (cm^{-1})		
Monomer	P6NI	Assignment
3332	3351	N—H stretching vibration
1585	1585	N—H elongation and deformation vibration
1618	1618	C=C stretching vibration on indole ring
1329	1329	NO_2 stretching vibration
865	877	Skeletal vibration of the benzene ring
814	814	C—H out-of-plane bending typical of 1,2,4-substituted benzene bring[30]
767	Absent	C_2—H out-of-plane deformation[30]
730	Weaker	C_3—H, C_4—H out-of-plane deformation[30]

N—H bonds on the doped P6NI main chain. Thus, the nitrogen centers could not be the polymerization sites. From Table I, it can also be seen that the benzene ring of the polymer remains intact after the electrochemical polymerization and is 1,2,4-trisubstituted. All these indications imply that the polymerization of 6-nitroindole mainly occurred at the 2,3-positions.

To further elucidate the polymer structure and the polymerization mechanism of 6-nitroindole, the ^{1}H-NMR spectrum of doped P6NI obtained from BFEE containing 10% EE was recorded and is illustrated in Figure 6(B). For comparison, the ^{1}H-NMR spectrum of the monomer is shown in Figure 6(A). The proton resonances of P6NI [Fig. 6(B)] are much broader than the corresponding proton resonances of 6-nitroindole [Fig. 6(A)] because of the wide molar mass distribution or complex structure of P6NI. The displacement of the chemical shifts of the polymer toward a lower field reflects the higher conjugation length in comparison with the monomer.[64] Six proton groups can be discerned in the ^{1}H-NMR spectrum of 6-nitroindole (δ = 6.54 ppm, δ = 7.64 ppm, δ = 7.72 ppm, δ = 7.81 ppm, δ = 8.27 ppm, and δ = 11.80 ppm), and they can be assigned to the protons at positions *b*, *a*, *c*, *d*, *e*, and *f*, respectively [Fig. 6(A)]. Because of the spin–spin splitting between the protons at positions *c* and *a* and *c* and *d*, these resonances appear as multiplets [Fig. 6(A)]. The chemical shifts of δ = 11.92 ppm, δ = 12.06 ppm, and δ = 12.36 ppm [Fig. 6(B)] can be assigned to the proton at position *f* of the N—H bond in P6NI. This means that the N—H bond is still present on the main chain of the polymer. The chemical shifts of δ = 8.5–8.71 ppm, δ = 8.16–8.29 ppm, and δ = 8.0–8.10 ppm can be assigned to the protons at positions *e*, *d*, and *c*, respectively [Fig. 6(B)]. This implies that the polymerization sites were the *a*,*b*-positions (C_2 and C_3), in good accordance with the IR results. The probable polymerization reaction of 6-nitroindole is illustrated in Scheme 1.

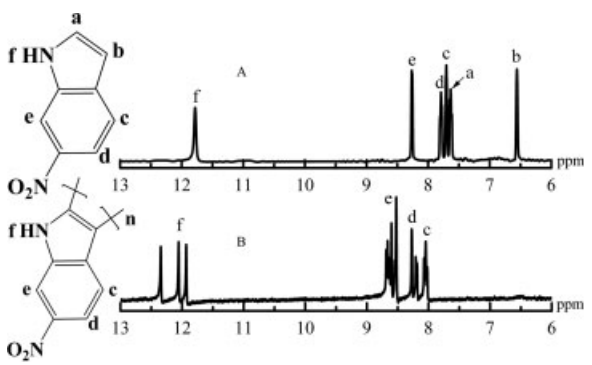

Figure 6 ^{1}H-NMR spectra of (A) 6-nitroindole and (B) doped P6NI obtained potentiostatically at 1.23 V versus SCE from BFEE containing 10% EE. The solvent was DMSO-d_6.

The fluorescence spectra of 6-nitroindole monomer and dedoped P6NI prepared in BFEE containing 10% EE were examined in THF solutions through excitation and emission wavelength scans, as shown in Figure 7. The peak of the excitation spectrum of the monomer is at 280 nm, and the peak of the emission spectrum is around 303 nm. On the contrary, the peak of the excitation spectrum of dedoped P6NI is at 416 nm, whereas the emission spectrum peak is around 535 nm. This implies that there is a large bathochromic shift in the excitation and emission wavelengths between the monomer and the polymer. The redshift of the emission peak further proved the formation of the conjugated backbone of P6NI, in good agreement with the UV–vis spectral results (Fig. 4). These results demonstrate that P6NI may be a candidate for use in green-light-emitting materials. The fluorescence quantum yield of as-

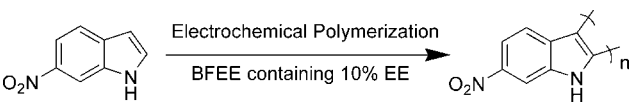

Scheme 1 Electrochemical polymerization of 6-nitroindole.

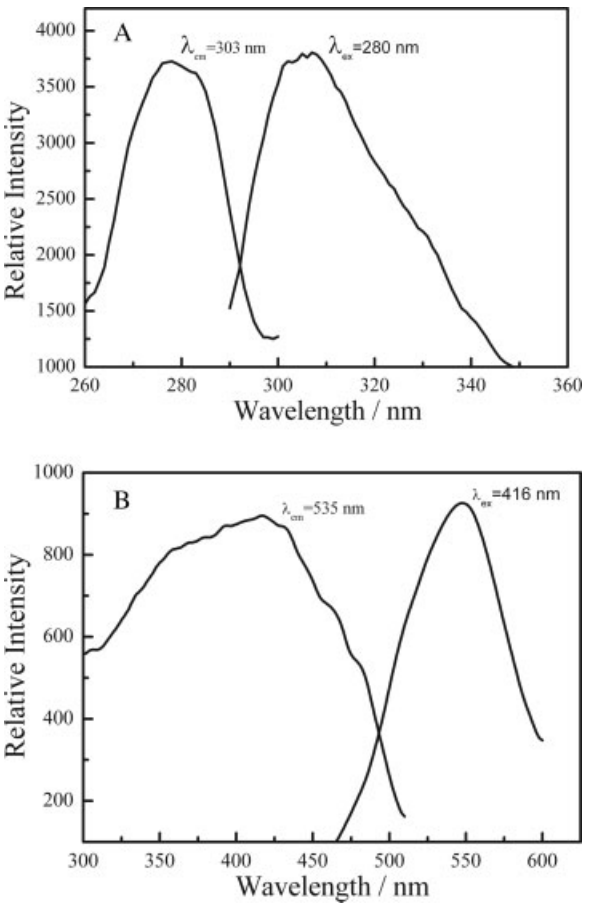

Figure 7 Excitation–emission spectra of (A) monomer 6-nitroindole and (B) dedoped P6NI in THF.

formed P6NI in THF was measured to be 0.05 according to eq. (1).

Thermal analysis

The thermal stability of conducting polymers is very important with respect to their potential applications. TGA is a significant dynamic way of detecting degradation behavior. The weight loss of a polymer sample is measured continuously while the temperature is changed at a constant rate. To investigate the thermal stability of P6NI films prepared in BFEE containing 10% EE, dedoped P6NI was thermally analyzed in this way (Fig. 8). The thermal analysis was performed under a nitrogen stream in the temperature range of 280–1059 K at a heating rate of 10 K/min. As shown in Figure 8, there was slight weight loss from 280 to 473 K, amounting to 7.1%. This degradation can be ascribed to the evaporation of water or other volatiles trapped in the polymer.[65] Decomposition amounting to 27.1% occurred between 473 and 627 K. This weight loss may be attributed to degradation of the skeletal P6NI backbone chain structure. In addition, there was still evident decomposition, amounting to about 9.3%, between 627 and 772 K, possibly due to the overflow of some oligomers that decomposed from P6NI with increasing temperature. The final weight loss was about 56.5% from 772 to 1059 K, possibly because of the ashing of carbon. From the differential thermogravimetry (DTG) curve [Fig. 8(B)], it can be seen that the rate of weight loss from P6NI was fastest at a temperature of 528 K. These results indicate good thermal stability of the P6NI films obtained from BFEE containing 10% EE.

Morphology and conductivity

SEM images of a P6NI film prepared from BFEE containing 10% EE are shown in Figure 9. The surface of the doped P6NI film is very smooth and dense [Fig. 9(A,B)]. However, the dedoped P6NI film shows several holes on its surface [Fig. 9(C,D)]. This can be ascribed to the displacement of the counteranion out of the P6NI film. These observations confirm the movement of doping anions into and out of the polymer film during doping and dedoping, in good agreement with the redox activity of the P6NI films.

The electrical conductivity of pressed pellets of doped P6NI obtained from BFEE containing 10% EE was measured to be 0.08 S/cm.

CONCLUSIONS

P6NI films with an electrical conductivity of 0.08 S/cm were electrochemically synthesized by direct anodic oxidation of 6-nitroindole in BFEE containing 10% EE. The oxidation potential of 6-nitroindole in this medium was determined to be just 0.98 V versus an SCE, which is much lower than that determined in CH_3CN containing 0.1 mol/L Bu_4NBF_4 (1.6 V vs

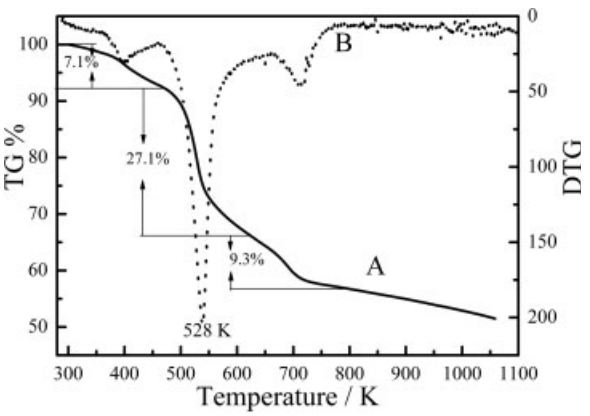

Figure 8 TGA curves of dedoped P6NI films obtained potentiostatically at 1.23 V versus SCE from BFEE containing 10% EE after treatment with 25% aqueous ammonia for 3 days.

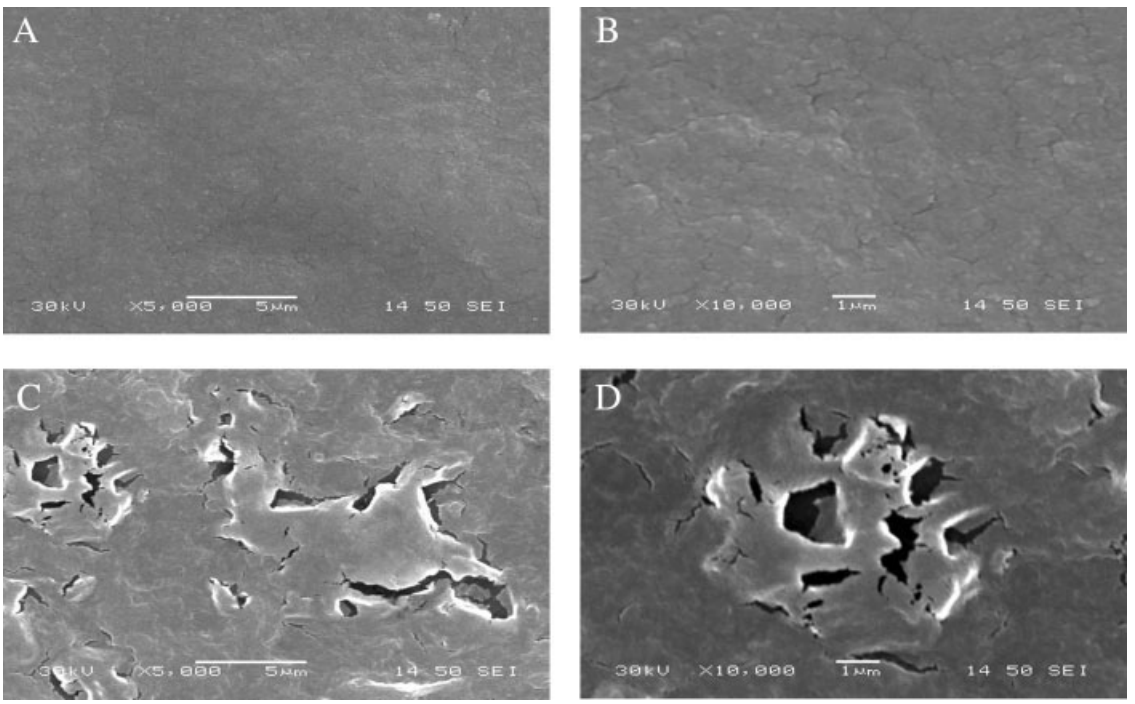

Figure 9 SEM micrographs of films deposited on an ITO glass electrode surface from BFEE containing 10% EE at an applied constant potential of 1.23 V versus SCE: (A,B) doped and (C,D) dedoped.

SCE). According to IR and ^{1}H-NMR spectra, P6NI was grown mainly as a result of coupling of the monomer at the C_2 and C_3 positions. TGA results indicated good thermal stability of the P6NI films obtained from BFEE containing 10% EE. The fluorescence quantum yield of as-formed P6NI in THF was measured to be 0.05.

References

1. Handbook of Conducting Polymers, 2nd ed.; Skotheim, T. A.; Elsembaumer, R. L.; Reynolds, J. R., Eds.; Marcel Dekker: New York, 1998.
2. Novak, P.; Muller, K.; Santhanam, K. S. V. Chem Rev 1997, 97, 207.
3. Wan, X. M. Polym Bull (in Chinese) 1999, 3, 50.
4. Biallozor, S.; Kupniewska, A. Synth Met 2005, 105, 443.
5. Gurunathan, K.; Murugan, A. V.; Marimuthu, R.; Mulik, U. P.; Amalnerkar, D. P. Mater Chem Phys 1999, 61, 173.
6. Groenendaal, L. B.; Zotti, G.; Aubert, P. H.; Waybright, S. M.; Reynolds, J. R. Adv Mater 2003, 15, 855.
7. Ghita, M.; Arrigan, D. W. M. Electrochim Acta 2004, 49, 4743.
8. Suematsu, S.; Ishikawa, T.; Hanada, M.; Takenouchi, H.; Naoi, K. Electrochemistry (in Japanese) 2003, 71, 695.
9. Sazou, D. Synth Met 2002, 130, 45.
10. Billaud, D.; Maarouf, E. B.; Hannecart, E. Mater Res Bull 1994, 29, 1239.
11. Billaud, D.; Maarouf, E. B.; Hannecart, E. Synth Met 1995, 69, 571.
12. Pandey, P. C.; Prakash, R. J Electrochem Soc 1998, 145, 4103.
13. Abthagir, P. S.; Dhanalakshmi, K.; Saraswathi, R. Synth Met 1998, 93, 1.
14. Maarouf, E. B.; Billaud, D.; Hannecart, E. Mater Res Bull 1994, 29, 637.
15. Lazzaroni, R.; DePryck, A.; Debraisieux, C. H.; Riga, J.; Verbist, J.; Brédas, J. L.; Delhalle, J.; André, J. M. Synth Met 1987, 21, 187.
16. Yurtsever, M.; Yurtsever, E. Polymer 2002, 43, 6019.
17. Choi, K. M.; Kim, C. Y.; Kim, K. H. J Phys Chem 1992, 96, 3782.
18. Talbi, H.; Billaud, D. Synth Met 1998, 93, 105.
19. Tourillon, G.; Garnier, F. J Electroanal Chem 1982, 135, 173.
20. Waltman, R. J.; Diaz, A. F.; Bargon, J. J Phys Chem 1984, 88, 4343.
21. Jackowska, K.; Kudelski, A.; Bukowska, J. Electrochim Acta 1994, 39, 1365.
22. Talbi, H.; Humbert, B.; Billaud, D. Synth Met 1997, 84, 875.
23. Talbi, H.; Ghanbaja, J.; Billaud, D. Polymer 1997, 38, 2099.
24. Zotti, G.; Zecchin, S.; Schiavon, G. Chem Mater 1994, 6, 1742.
25. Pandey, P. C.; Prakash, R. Sens Actuators B 1998, 46, 61.
26. Pandey, P. C.; Prakash, R. J Electrochem Soc 1998, 145, 999.
27. Longchamp, S.; Caullet, C. Electrochim Acta 1984, 29, 1075.
28. Talbi, H.; Monard, G.; Loos, M.; Billaud, D. Synth Met 1999, 101, 115.
29. Dhanalakshmi, K.; Saraswathi, R. J Mater Sci 2001, 36, 4107.
30. Talbi, H.; Humbert, B.; Billaud, D. Spectrochim Acta A 1998, 54, 1879.
31. Wan, F.; Li, L.; Wan, X.; Xue, G. J Appl Polym Sci 2002, 85, 814.
32. Choi, K. M.; Jang, J.; Rhee, H. H.; Kim, K. H. J Appl Polym Sci 1992, 46, 1695.
33. Tüken, T.; Düdükçü, M.; Yazıcı, B.; Erbil, M. Prog Org Coat 2004, 50, 273.
34. Van Mullekom, H. A. M.; Vekemans, J. A. J. M.; Havinga, E. E.; Meijer, E. W. Mater Sci Eng R 2001, 32, 1.
35. Brocks, G.; Tol, A. J Phys Chem 1996, 100, 1838.
36. Brocks, G.; Tol, A. Synth Met 1996, 76, 213.
37. Gronenendall, L. B.; Jonas, F.; Freitga, D.; Pielartzik, H.; Reynolds, J. R. Adv Mater 2000, 12, 481.
38. Kumar, D.; Sharma, R. C. Eur Polym J 1998, 34, 1053.
39. Roncali, J. Chem Rev 1992, 92, 711.

40. Shi, G. Q.; Jin, S.; Xue, G.; Li, C. Science 1995, 267, 994.
41. Shi, G. Q.; Li, C.; Liang, Y. Q. Adv Mater 1999, 11, 1145.
42. Li, C.; Shi, G. Q.; Liang, Y. Q. J Electroanal Chem 1998, 455, 1.
43. Huang, Z.; Qu, L.; Shi, G. Q.; Chen, F.; Hong, X. J Electroanal Chem 2003, 556, 159.
44. Li, C.; Shi, G. Q.; Liang, Y. Q.; Ye, W.; Sha, Z. Polymer 1997, 38, 5023.
45. Wang, X.; Shi, G. Q.; Liang, Y. Electrochem Commun 1999, 1, 536.
46. Xu, J.; Nie, G.; Zhang, S.; Hou, J.; Han, X.; Pu, S. J Polym Sci Part A: Polym Chem 2005, 43, 1444.
47. Wan, X.; Lu, Y.; Liu, X.; Zhou, L.; Jin, S.; Xue, G. Chin J Polym Sci 1999, 17, 99.
48. Xu, J.; Shi, G.; Qu, L.; Zhang, J. Synth Met 2003, 135, 221.
49. Liu, C.; Zhang, J.; Shi, G.; Zhao, Y. J Phys Chem B 2004, 108, 2195.
50. Wan, X.; Yan, F.; Jin, S.; Liu, X.; Xue, G. Chem Mater 1999, 11, 2400.
51. Li, C.; Shi, G.; Liang, Y. Synth Met 1999, 104, 113.
52. Bazzaoui, E. A.; Aeiyach, S.; Lacaze, P. C. Synth Met 1996, 83, 159.
53. Goldenberg, L. M.; Aeiyach, S.; Lacaze, P. C. Synth Met 1993, 55, 1360.
54. Gningue-Sall, D.; Fall, M.; Dieng, M. M.; Aaron, J. J.; Lacaze, P. C. Phys Chem Chem Phys 1999, 1, 1731.
55. Zimmermann, C.; Mohr, M.; Zipse, H.; Eichberger, R.; Schnabel, W. J Photochem Photobiol A Chem 1999, 125, 47.
56. Tasi, F. C.; Chang, C. C.; Liu, C. L.; Chen, W. C.; Jenekhe, S. A. Macromolecules 2005, 38, 1958.
57. Xu, J. K.; Liu, H. T.; Pu, S. Z.; Li, F. Y.; Luo, M. B. Macromolecules 2006, 39, 5611.
58. Tanaka, K.; Shichiri, T.; Wang, S.; Yamabe, T. Synth Met 1988, 24, 203.
59. Du, X.; Wang, Z. Electrochim Acta 2003, 48, 1713.
60. Otero, T. F.; Larreta-Azelain, E. D. Polymer 1988, 29, 1522.
61. Sak-Bisnar, M.; Budimir, M.; Kovac, S.; Kukulj, D.; Duic, L. J Polym Sci Part A: Polym Chem 1992, 30, 1609.
62. Talbi, H.; Maarouf, E. B.; Humbert, B.; Alnot, M.; Ehrhardt, J.; Ghanbaja, J.; Billaud, D. J Phys Chem Solids 1996, 57, 1145.
63. Saraji, M.; Bagheri, A. Synth Met 1998, 98, 57.
64. Xu, J. K.; Hou, J.; Zhou, W. Q.; Nie, G. M.; Pu, S. Z.; Zhang, S. S. Spectrochim Acta A 2006, 63, 723.
65. Thieblemont, J. C.; Brun, A.; Marty, J.; Planche, M. F.; Calo, P. Polymer 1995, 36, 1605.